

Identifying a new intermediate-polar using XMM-Newton and INTEGRAL

Matthew J. Middleton¹, Edward M. Cackett², Craig Shaw¹, Gavin Ramsay³,
 Timothy P. Roberts¹ and Peter J. Wheatley⁴

¹*Department of Physics, University of Durham, South Road, Durham DH1 3LE, UK*

²*Institute of Astronomy, University of Cambridge, Madingley Road, Cambridge CB3 0HA, UK*

³*Armagh Observatory, College Hill, Armagh BT61 9DG*

⁴*Department of Physics, University of Warwick, Coventry CV4 7AL, UK*

7 December 2017

ABSTRACT

The bright X-ray source, 2XMMi J180438.7-145647 is fortunate to have long baseline observations in *INTEGRAL* that compliment observations taken by other missions. Optical spectroscopy of this object has suggested a distance of ~ 7 kpc and an identification with a low mass X-ray binary. We instead use the X-ray data from 0.3–40 keV to identify the source as a bright intermediate polar (IP) with an estimate for the white dwarf mass of $\sim 0.60 M_{\odot}$. This identification is supported by the presence of an iron triplet, the component lines of which are some of the strongest seen in IPs; and the signature of the spin period of the white dwarf at ~ 24 mins. We note that the lack of broad-band variability may suggest that this object is a stream-fed IP, similar in many respects to the well studied IP, V2400 Oph. Phase-binning has allowed us to create spectra corresponding to the peaks and troughs of the lightcurve from which we determine that the spectra appear harder in the troughs, consistent with the behaviour of other IPs binned on their spin periods. This work strongly suggests a mis-identification in the optical due to the presence of large columns of enshrouding material. We instead propose a distance to the source of < 2.5 kpc to be consistent with the luminosities of other IPs in the dim, hard state. The relatively high flux of the source together with the strength of the iron lines may, in future, allow the source to be used to diagnose the properties of the shock heated plasma and the reflected component of the emission.

Key words: accretion, accretion discs – novae, cataclysmic variables – X-rays: binaries

1 INTRODUCTION

Cataclysmic variables (CVs) populate the central-to-faint section of the galactic X-ray luminosity function (10^{31-34} erg s^{-1} , see Sazonov et al. 2006) and may provide a substantial percentage of the hard X-ray emission seen in the galactic ridge (Revnivtsev et al. 2009). In such systems, accretion from a low-mass donor star (Cowley et al. 1998 but see also Orio et al. 2010) onto the white dwarf (WD) may occur via either an accretion disc (Shakura & Sunyaev 1973) or via columns of material following the WD’s magnetic field lines and impacting the poles. The latter system is dubbed a polar or intermediate polar (IP) system dependent upon the magnetic field strength and the emission is typified by cooling of shock-heated gas near the WD surface (see Cropper

1990 for a review of polars) and imprinted absorption and emission features.

Such systems may be seen to enter a nova outburst state where the material builds up on the surface of the WD leading to thermo-nuclear burning (Pietch et al. 2005). The observational result of a nova is a super-soft source (SSS) but following this they enter a persistent and much dimmer, harder state (although the long-term behaviour can also include brighter episodes due to dwarf-novae from disc instabilities, e.g. Idan et al. 2010). The highest luminosity of this low-state has been attributed to GK Persei ($\sim 1.1 \times 10^{34}$ erg s^{-1} in a 2006 outburst) although there is still uncertainty in its distance (~ 340 pc - Warner 1987 to 525 pc - Duerbeck 1981) and this is potentially exceeded by a CV in M3

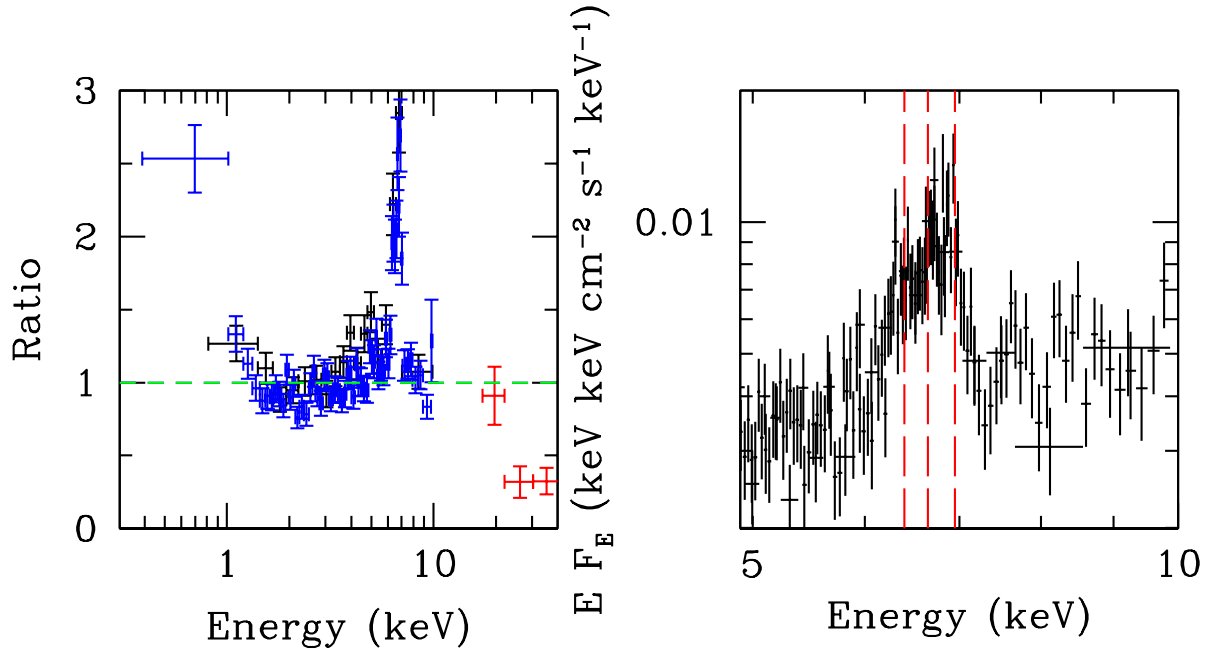


Figure 1. *Left:* ratio of the *XMM-Newton* (PN: blue, and MOS1: black) and *INTEGRAL* data (ISGRI: red) to a model of an absorbed power-law with a best-fitting index of ~ 0.94 . There are clear, strong residuals due to iron emission and the presence of a roll-over in the spectrum below ~ 20 keV. *Right:* The *XMM-Newton* data from 5–10 keV (unfolded through a power-law of $\Gamma=0$ and $\text{norm}=1$) together with dashed vertical lines indicating the rest-frame energies for the iron triplet (6.4, 6.65 and 6.95 keV respectively).

(1E1339 with a luminosity of $\sim 1.4 \times 10^{34}$ erg s^{-1} - Stacey et al. 2011).

A further feature of such objects is the presence of periodicity in the X-ray and optical lightcurves indicating either the orbital period of the secondary (from the optical emission) ranging from ~ 1.4 - 50 hours (Hilton et al 2009; Crampton et al. 1986) or the spin period of the WD, taking values between ~ 30 s (de Jager et al. 1994) and ~ 4000 s (Mauche et al. 2009).

In this letter we present the discovery of a new, persistent, IP using both *INTEGRAL* and *XMM-Newton* data to constrain the important spectral and timing characteristics. We explore the uncertainty in the distance estimate to this object based on the optical spectroscopy presented by Masetti et al. (2008) and find that the estimate of 7 kpc is probably incorrect given the absorbing material expected to be present in such systems.

2 DATA AND PREVIOUS ANALYSIS

The IR source, 2MASS J180438.92-145647.4 has been identified by the *INTEGRAL* Galactic survey as a hard, X-ray bright source of interest. Two optical investigations have followed, first by Burenin et al. (2006) who identify the counterpart as a massive star and Masetti et al. (2008) who identify it as a low mass star. The latter assume that the extinction of 3 magnitudes from optical line ratios is incorrect due to the large inferred distances that would result and instead determine a distance of ~ 7 kpc (based on the Galactic colour excess). This suggests that the source is one of the very faintest low-mass X-ray binaries (LMXBs) and

likely to therefore be a member of the very-faint X-ray transients (VFXTs see Munro et al. 2005b; Sakano et al. 2005; Wijnands et al. 2006; Degenaar & Wijnands 2009). However, the optical magnitude (18.7 in the R band) together with 3 magnitudes of absorption would suggest an identification of the secondary with a giant star and therefore a high-mass X-ray binary (HMXB). If this is the case then the distance estimate of 7 kpc would make it extremely faint (only $\sim 1 \times 10^{35}$ erg s^{-1}) for a HMXB (e.g. Grimm, Gilfanov & Sunyaev 2006), and would imply that we are looking at an object even more distant and on the far side of the galactic bulge.

The source has been observed in the 0.2–10 keV X-ray band on three occasions, a short (1ks) *Chandra* positional pointing (OBSID: 7275), a ~ 12 ks pointed observation by *XMM-Newton* (OBSID: 0405390301, identifier: 2XMMi J180438.7-145647) and a followup *Swift* ToO (taken 9th March 2011) which has confirmed that the source is persistent, thus effectively ruling out an identification with the subset of VFXTs. The source has also been observed by the higher energy X-ray detectors on-board *INTEGRAL* for a sum exposure time of ~ 2500 ks taken over several years overlapping with the *XMM-Newton* observation. Given its proven persistent nature and the simple fact that the source would not be detected in the higher energy bandpass if in short-lived outburst (i.e. when a SSS), we include the data in our analysis as a contemporaneous description of the emission above 10 keV.

We extract the *XMM-Newton* data using SAS v10 and filter the imaging data using standard patterns (≤ 4 for PN and ≤ 12 for the MOS) and flags ($\text{==}0$). We proceed to remove hard proton flaring episodes from the full-field

high energy (>10 keV) lightcurve, leaving ~ 10 ks of good data (this is the most conservative estimate of the good time interval, the source is actually much brighter than the background <10 keV for the full observation length of ~ 12.6 ks), and proceed to extract spectra using XSELECT from circular source and background regions of $35''$ radius. Although the MOS2 central chip was turned off for the duration of the observation, both the MOS1 and PN were exposed for the full duration.

3 X-RAY SPECTRAL ANALYSIS

We fit the background subtracted *XMM-Newton* data (grouped on a minimum of 25 counts per energy channel) together with the standard spectral *INTEGRAL* (ISGRI) products in XSPEC v 11.3.2 with a simple power-law, absorbed by a neutral foreground column and a constant of proportionality to account for differences between the detector responses (in XSPEC this is `CONST*TBABS*POW`). The resulting fit quality is very poor (χ^2 of 858.7 for 330 d.o.f.).

The reason for this poor fit is clear from the ratio plot shown in Figure 1. Whilst the extremely hard ($\Gamma = 0.94^{+0.05}_{-0.03}$) power-law is a good description of the underlying continuum below ~ 6 keV (except at the lowest energies where there appears to be a soft excess), there is a large, broad iron emission feature followed by an obvious roll-over below ~ 20 keV. Adding a single Gaussian dramatically improves the fit quality ($\Delta\chi^2 \sim 345$ for 3 d.o.f.) giving a broad ($\sigma = 0.35$ keV) and strong (equivalent width (EQW) of ~ 1.4 keV) line which peaks at 6.64 keV. The breadth of the line could be due to smeared reflection as seen in X-ray binaries (XRBs) at low mass accretion rates (see Fabian 2005) however, the spectral properties are inconsistent and the EQW of this feature is far larger than has been seen in any reflection dominated XRB to date, suggesting an alternative origin. Instead we obtain a marginally better fit ($\Delta\chi^2 \sim 12$ for 6 d.o.f.) by describing the excess as an iron triplet corresponding to lab-frame energies of ~ 6.4 , 6.65 and 6.95 keV. Together with the underlying hard continuum ($\Gamma \sim 1.00 \pm 0.05$), we then initially identify the source as an IP in the persistent dim, hard state (rather than a polar candidate as the spectrum is too hard to be described by cyclotron emission: Cropper 1990). In this case we would expect the spectrum to be dominated by Bremsstrahlung cooling with a strong component of photo-electric absorption (Norton & Watson 1989) and reflected emission from the WD surface creating the strong iron $K\alpha$ line (Beardmore et al. 1995; Done, Osborne & Beardmore 1995; Done & Magdziarz 1998).

Although a good physical description is one of a multi-temperature model for the plasma, generally speaking the data quality of IPs is not high enough to distinguish this from a single temperature plasma model. We therefore assume a simple, single temperature description of the plasma flow, and create a model comprising a cooling flow plasma, reflection from the surface of the WD (with a fixed incident spectral index of 1.5) all of which is obscured by a neutral partial covering fraction and a foreground Galactic column¹ (in XSPEC this

is `CONST*TBABS*PCFABS*(REFXION†(CVMEKAL‡))`). We find the requirement for a second neutral covering fraction ($\Delta\chi^2 \geq 100$ for 2 d.o.f.) although the inclusion of any further absorbers does not significantly improve the fit. We obtain a good description of the data (χ^2 of 346.5 for 325 d.o.f.) with the best-fitting model and residuals plotted together in Figure 2 and the model parameters with 90% confidence limits provided in Table 1 (note that, in this best-fitting case, the constants of proportionality are consistent within 10% of unity). The model provides an estimate for the unabsorbed 0.3-10 keV flux of 2.4×10^{-11} ergs cm^{-2} s^{-1} . This is very bright for an IP in the dim, hard state (although a distance of ~ 2.5 kpc would be required in order for this to be the brightest: Stacey et al. 2011). However, whilst the source is relatively bright, the hard continuum precludes a useful RGS analysis which could identify soft emission/absorption features (and identify the multi-temperature nature of the emission: Wu et al. 2003).

The strong iron feature in the spectrum (see Fig. 1) may be well described by a combination of 3 Gaussians (although the 6.4 keV line originates from reflection from the WD surface rather than intrinsic photo-electric emission from the plasma) and we obtain the properties of these by fitting the *XMM-Newton* data alone together with a simple absorbed power-law continuum. The best-fitting model parameters are also shown in Table 1. These show that, whilst the properties of the continuum are consistent with those seen for other IPs, the inferred equivalent widths (EQW) of the iron lines are towards the upper limit of what has previously been observed (e.g. Butters et al. 2011). We note that, due to the marginal improvement in fit quality from including 3 Gaussians over a single component, obtaining constraining estimates for the errors on the strength (EQW) and breadth (σ) is unrealistic and so are omitted.

To ensure that cross-calibration errors are not overly influencing the best-fitting model parameters, we test the upper and lower limits for the constant of proportionality to the *INTEGRAL* data ($\sim 1.03 \pm 0.4$ - consistent with the cross-calibration status of EPIC versus ISGRI²). In both cases, we obtain values for the temperature of the rollover within the 90% confidence limits presented in Table 1. This rollover in the spectrum, due to the mean temperature of the plasma emission, can then be used as a crude measure for the mass of the WD. Aizu (1973) gives a formula relating the gravitational potential of the WD to the mass and radius:

$$kT_s = 16 \times \left(\frac{M}{0.5M_\odot} \right) \left(\frac{R}{10^9 \text{cm}} \right)^{-1} \text{keV} \quad (1)$$

Substituting the analytical expression for the radius (Nauenberg 1972):

$0.6 \times 10^{22} \text{cm}^{-2}$ to be consistent with the estimates available from HEASARC (Dickey & Lockman 1990; Kalberla et al. 2005)

[†] This is a private model based on REFLBAL as described in Done & Gierliński (2006) but with the updated ionisation tables of Ross & Fabian (2005).

[‡] See Singh et al. (1996).

² See Kirsch et al. (2004) and http://heasarc.nasa.gov/docs/heasarc/caldb/caldb_xcal.html. For examples of this in use see e.g. Caballero-García et al. (2009)

¹ We use an extrinsic column with an upper limit of

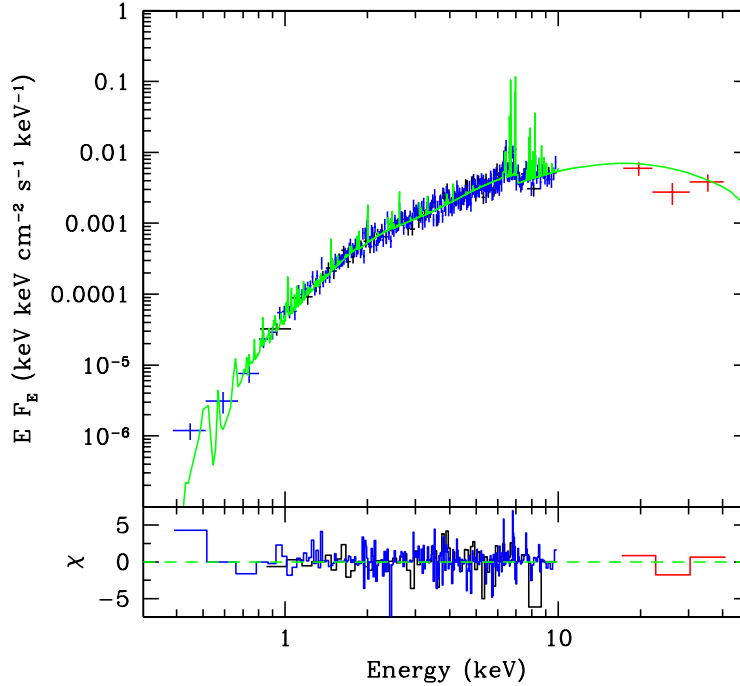


Figure 2. X-ray spectral data from the PN (blue) and MOS1 (black) together with the *INTEGRAL* ISGRI data (red). The best fitting model comprising a cooling flow, reflection and absorption (see Table 1) is shown in green with residuals to this in the panel below.

$$R = 0.78 \times 10^9 \left[\left(\frac{1.44 M_{\odot}}{M} \right)^{\frac{2}{3}} - \left(\frac{M}{1.44 M_{\odot}} \right)^{\frac{2}{3}} \right]^{\frac{1}{2}} \text{ cm} \quad (2)$$

allows us to calculate the mass of the WD from the shock temperature:

$$\frac{M_{\text{WD}}}{M_{\odot}} = 1.44 \times \left[\frac{1}{2} \left(1 + \sqrt{1 + 4 \times \left(\frac{59}{kT_s} \right)^2} \right) \right]^{-\frac{3}{4}} \quad (3)$$

Taking the best-fitting value for kT_s from our model ($23.30^{+8.84}_{-5.09}$ keV), this gives a mass of $0.62^{+0.13}_{-0.09} M_{\odot}$ assuming a single temperature description of the cooling flow. Based on the correction factor expected from the change in the gravitational potential over the shock height (Cropper et al. 1998, 1999) this provides an estimate for the mass of $\sim 0.60 M_{\odot}$, consistent with the median mass of isolated WDs (Kepler et al. 2007). It should be noted however that this assumes a single-temperature description whereas a physical model may well place the peak shock temperature above this (Cropper et al. 1999).

An important consequence as this identification is that there is a clear prediction for the presence of large columns of material that obscure the intrinsic emission (see Cropper et al. 1990). This therefore makes any associated optical identification and distance estimate based on line spectra highly unreliable as the intervening material will distort the emission. Instead, in order for the source to have similar luminosities to those of other IPs in the dim, hard state, we expect the distance to be < 2.5 kpc.

4 TIMING ANALYSIS

There is a wealth of evidence suggesting the presence of periodicities from the optical and X-ray lightcurves of IPs, attributed to either the orbital period of the secondary or the spin period of the WD³. The properties of the broad-band noise on which these periodicities sit in the power density spectrum (PDS) has been of great interest as the behaviour can provide observational tests for theories of how non-linear variability is generated in the accretion process (see e.g. the discussion of Uttley, McHardy & Vaughan 2005). In the case of XRBs, this is now widely accepted to be due to propagating fluctuations in the disc (see Lyubarskii 1997, Arévalo & Uttley 2006, Ingram & Done 2011). However, in the case of IPs, the inner regions of the inflow are disrupted by the magnetic field of the WD, leading to a large truncation radius of the accretion disc, within which, the material follows the magnetic field lines. There is therefore the prediction of a break in the PDS (beyond which the red noise follows $\sim \nu^{-2}$: Revnivtsev et al. 2010) which has now been observationally confirmed (Revnivtsev et al. 2009, 2010). Due to this break at low frequencies there is very little rapid variability, unlike in the cases of XRBs where significant rapid variability can be created by the magneto-rotational instability (MRI, see Beckwith, Armitage & Simon 2011) being established in a low density flow (Done, Gierliński & Kubota 2007). In the cases where the accretion flow is stream-fed (e.g. V2400 Oph), the lack of broad-band noise is evidently due to the observational lack of an accretion disc (Hellier & Beardmore

³

<http://asd.gsfc.nasa.gov/Koji.Mukai/iphome/catalog/members.html>

Table 1. Best fitting spectral parameters

CONS*TBABS ₁ *PCFABS ₁ *PCFABS ₂ (REFXION(CVMEKAL))		
$n_{H,1}$ ($\times 10^{22} \text{cm}^{-2}$)	28.02	$+8.51$ -6.88
Fraction ₁	0.67	$+0.05$ -0.06
$n_{H,2}$ ($\times 10^{22} \text{cm}^{-2}$)	1.85	$+0.42$ -0.40
Fraction ₂	0.80	$+0.06$ -0.03
$\log \xi$	1.00	$+0.77$ $-peg$
kT_{max} (keV)	23.30	$+8.84$ -5.09
Fe abund	0.67	$+0.25$ -0.17
χ^2 (d.o.f.)	346.8	(324)
Null P	0.18	
CONS*TBABS(POWERLAW+GAUSS ₁ +GAUSS ₂ +GAUSS ₃)		
$n_{H,1}$ ($\times 10^{22} \text{cm}^{-2}$)	0.81	$+0.06$ -0.07
Line energy ₁ (keV)	6.41	± 0.06
EQW ₁ (eV)	244	
σ_1 (keV)	0.16	
Line energy ₂ (keV)	6.69	± 0.04
EQW ₂ (eV)	99	
σ_2 (keV)	3.8×10^{-4}	
Line energy ₃ (keV)	6.91	± 0.05
EQW ₃ (eV)	324	
σ_3 (keV)	7.2×10^{-2}	
Γ	0.67	± 0.05
norm	3.2×10^{-4}	$\pm 0.2 \times 10^{-4}$
χ^2 (d.o.f.)	353.7	(316)
Null P	0.07	

Notes: The best-fitting parameter values are given with 90% confidence limits with the properties of the iron lines obtained separately to those of the continuum. Note that the ionisation parameter ($\log \xi$) is set to peg at a lower limit of 1.

2002). The position of the truncation radius and the nature of the accretion are therefore paramount in accurately determining the presence of periodicities. For example, where the disc truncates at very large radii (i.e. effectively stream-fed) there is the prediction that, at high frequencies, there should be little or no red noise in the PDS making significance tests here rather ambiguous (see the discussion of Vaughan 2005). However, where the statistical quality of the data allows, and there is a clear (and stringently tested) lack of broad-band red noise, there may be an argument for a significance test to be carried out above the white noise. In such a situation, observing the behaviour of the spectra binned on the period may allow for a second order test (see following section).

Although we do not have any simultaneous optical data, the identification of an X-ray periodicity may help further constrain the identification with an IP. We extract the 0.3-10 keV, co-added (using the PN and MOS1 with the same start and stop times), background subtracted lightcurve binned on 10 s, using the same regions as the spectral analysis. As the source dominates the background emission throughout the observation, we use the full observation length in order to improve any variability constraints. We initially test the shape of the broad-band variability out to the longest available timescales using the most robust LS method available (Vaughan 2010) and find that the broad-band continuum is consistent with the white noise at the 3σ level (although we

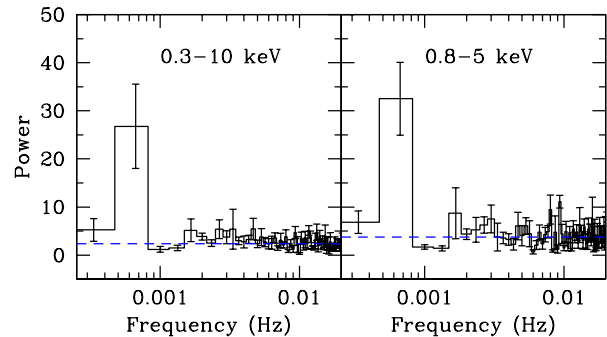


Figure 3. Average PDS extracted from the 0.3-10 keV (left) and 0.8-5 keV (right) lightcurves binned on 10 s, made from 5 segments of the lightcurve including the white noise (horizontal dashed line). There is an excess of variance at ~ 0.7 mHz which is significant at $>3\sigma$ in the 0.8-5 keV band. As the power over the remaining observable frequency bins is consistent with the statistical white noise (possibly indicating the source as being stream-fed) this is an acceptable method for determining the significance of this feature.

identify a possible peak of excess variance at ~ 0.7 mHz). Although we cannot probe down to very low frequencies, the fairly high data quality from this observation may imply that we should see variability power on these frequencies if there was a contribution from disc accretion (Revnivtsev et al. 2010). This suggests that we are observing a stream-fed IP similar to V2400 Oph (Norton, Haswell, & Wynn 2004) which is seen to possess a similar broad-band X-ray spectrum (Revnivtsev et al. 2004). This lack of broad-band noise therefore allows us to obtain tentative significance measurements assuming a white noise description of the continuum variability. We proceed to extract the power density spectrum (PDS) using the FTOOL: POWSPEC in units of fractional rms^2 . We extract the PDS averaged over 5 segments of the lightcurve in order to realistically constrain any bins of variability. We again find an excess of variance at ~ 0.7 mHz with the tightest constraints in the 0.8-5 keV band at a significance $>3\sigma$ (see Fig. 3). We note that the coherence of this excess variance (ν_{QPO}/ν_{FWHM}) is rather low, preventing a robust identification with a period/quasi-period (although the behaviour of the broad-band noise is unlikely to facilitate an identification with a break in the PDS), however a ~ 24 min period could be readily associated with the spin period of the WD and is similar to that of V2306 Cyg (Norton et al. 2002) at similar flux levels.

4.1 Phase-binned spectroscopy

We can better confirm the nature of the excess variance by extracting the spectral properties in the peaks and troughs of the lightcurve. This phase-binned spectroscopy has been applied to a number of IPs with confirmed spin periods (e.g. Pekön & Balman 2010; Hellier et al. 1996; Done, Osborne & Beardmore 1995) and, in each case, the troughs are found to have harder spectra due to the changing proportions of reflection and absorption.

We follow a similar approach and extract PN spectra from epochs corresponding to the peaks and troughs en-

suring no overlap between the two and avoiding the flaring episodes as with the time-averaged spectroscopy. This gives a total exposure of 3.8 ks for the peaks and 5.7 ks for the troughs. To identify any changes in continuum shape, we apply a simple power-law model to both sets of data simultaneously ((TBABS(POWERLAW)) over the 0.3-6 keV band (to ignore the distorting effects of the iron emission). We obtain best-fitting spectral index values of $0.32^{+0.12}_{-0.12}$ and $0.57^{+0.15}_{-0.14}$ for the troughs and peaks respectively and an improvement in $\Delta\chi^2$ of ~ 4.8 for 1 d.o.f. over fixing the index to be the same in both. This allows us to claim that the spectrum of the troughs appears harder, consistent with the behaviour of other IPs in the dipping phase of their spin period. We attempt to quantify the changing properties of the iron emission by fixing the continuum to the best-fitting value below 6 keV and including 3 Gaussian components in the model. However, the much shorter exposure for each phase-binned spectrum prevents any difference from being well constrained.

5 CONCLUSION

The hard, bright X-ray source, 2XMMi J180438.7-145647, has been observed only once by *XMM-Newton*, however, together with the available *INTEGRAL* (ISGRI) data, this relatively short observation has shown that the time-averaged X-ray emission is characteristic of an IP. In general we determine similar properties for this source when we compare them with that of the wider population of IPs, save for the iron features which are notably strong. It is possible that any future, longer observation, may be able to use this strong iron triplet to provide a better diagnostic of the plasma region.

Due to the extremely hard X-ray spectrum and short observation length, we cannot obtain a useful RGS spectrum thus precluding a more complex (multi-temperature) description of the plasma. However, the inclusion of *INTEGRAL* (ISGRI) data has allowed us to place constraints on the mean temperature of the plasma cooling flow. Taking into account the changing gravitational potential over the shock height, this provides an estimate for the mass of the WD of $\sim 0.60 M_{\odot}$, consistent with the median of isolated WD masses.

We detect the presence of excess variance power at ~ 0.7 mHz which *may* be associated with the spin period of the WD. Phase-binning the emission produces spectra which show behaviour consistent with that of other IPs, supporting this identification for the source. The lack of variability apart from this feature suggests that we are observing a stream-fed IP, similar in behaviour to V2400 Oph.

Given the large columns of absorbing material enshrouding IPs, we find that the distance estimate based on the optical spectrum (Masetti et al. 2008) to be highly unreliable. Instead, given the flux of the source, its distance is much more likely to be < 2.5 kpc to be consistent with the observed luminosities of other IPs.

6 ACKNOWLEDGEMENTS

MM and TR thanks STFC for support in the form of a standard grant. This work is based on observations obtained with *XMM-Newton*, an ESA science mission with instruments and contributions directly funded by ESA Member States and NASA. This work also makes use of observations taken by *INTEGRAL*, an ESA project with instruments and science data centre funded by ESA member states (especially the PI countries: Denmark, France, Germany, Italy, Switzerland, Spain), Poland and with the participation of Russia and the USA. We also acknowledge support from Dr Tony Bird at the University of Southampton for his help with the *INTEGRAL* data products.

REFERENCES

- Aizu K., 1973, PThPh, 49, 1184
 Arévalo P., Uttley P., 2006, MNRAS, 367, 801
 Beardmore A. P., Done C., Osborne J. P., Ishida M., 1995, MNRAS, 272, 749
 Beckwith K., Armitage P. J., Simon J. B., 2011, arXiv, arXiv:1105.1789
 Burenin R., Mescheryakov A., Revnivtsev M., Bikmaev I., Sunyaev R., 2006, ATel, 880, 1
 Butters O. W., Norton A. J., Mukai K., Tomsick J. A., 2011, A&A, 526, A77
 Caballero-García M. D., Miller J. M., Trigo M. D., Kuulkers E., Fabian A. C., Mas-Hesse J. M., Steeghs D., van der Klis M., 2009, ApJ, 692, 1339
 Cowley A. P., Schmidtke P. C., Crampton D., Hutchings J. B., 1998, ApJ, 504, 854
 Crampton D., Fisher W. A., Cowley A. P., 1986, ApJ, 300, 788
 Cropper M., 1990, SSRv, 54, 195
 Cropper M., Ramsay G., Wu K., 1998, MNRAS, 293, 222
 Cropper M., Wu K., Ramsay G., Kocabişik A., 1999, MNRAS, 306, 684
 Degenaar N., Wijnands R., 2009, A&A, 495, 547
 de Jager O. C., Meintjes P. J., O'Donoghue D., Robinson E. L., 1994, MNRAS, 267, 577
 Dickey J. M., Lockman F. J., 1990, ARA&A, 28, 215
 Done C., Gierliński M., 2006, MNRAS, 367, 659
 Done C., Gierliński M., Kubota A., 2007, A&ARv, 15, 1
 Done C., Magdziarz P., 1998, MNRAS, 298, 737
 Done C., Osborne J. P., Beardmore A. P., 1995, MNRAS, 276, 483
 Duerbeck H. W., 1981, PASP, 93, 165
 Fabian A. C., 2005, Ap&SS, 300, 97
 Grimm H.-J., Gilfanov M., Sunyaev R., 2006, IAUS, 230, 353
 Hellier C., Mukai K., Ishida M., Fujimoto R., 1996, MNRAS, 280, 877
 Hellier C., Beardmore A. P., 2002, MNRAS, 331, 407
 Hilton E. J., Szkody P., Mukadam A., Henden A., Dillon W., Schmidt G. D., 2009, AJ, 137, 3606
 Idan I., Lasota J.-P., Hameury J.-M., Shaviv G., 2010, A&A, 519, A117
 Ingram A., Done C., 2011, MNRAS, 799
 Kalberla P. M. W., Burton W. B., Hartmann D., Arnal E. M., Bajaja E., Morras R., Pöppel W. G. L., 2005, A&A, 440, 775
 Kepler S. O., Kleinman S. J., Nitta A., Koester D., Castanheira B. G., Giovannini O., Costa A. F. M., Althaus L., 2007, MNRAS, 375, 1315
 Kirsch M. G. F., Becker W., Larsson S., Brandt S., Budtz-Jørgensen C., Westergaard N. J., Much R., 2004, ESASP, 552, 863
 Lyubarskii Y. E., 1997, MNRAS, 292, 679

- Masetti N., et al., 2008, *A&A*, 482, 113
- Mauche C. W., Brickhouse N. S., Hoogerwerf R., Luna G. J. M., Mukai K., Sterken C., 2009, *IBVS*, 5876, 1
- Muno M. P., Pfahl E., Baganoff F. K., Brandt W. N., Ghez A., Lu J., Morris M. R., 2005, *ApJ*, 622, L113
- Nauenberg M., 1972, *ApJ*, 175, 417
- Norton A. J., Haswell C. A., Wynn G. A., 2004, *A&A*, 419, 1025
- Norton A. J., Quaintrell H., Katajainen S., Lehto H. J., Mukai K., Negueruela I., 2002, *A&A*, 384, 195
- Norton A. J., Watson M. G., 1989, *MNRAS*, 237, 853
- Orio M., Nelson T., Bianchini A., Di Mille F., Harbeck D., 2010, *ApJ*, 717, 739
- Pekön Y., Balman S., 2011, *MNRAS*, 411, 1177
- Pietsch W., Fliri J., Freyberg M. J., Greiner J., Haberl F., Riffeser A., Sala G., 2005, *A&A*, 442, 879
- Revnivtsev M. G., Lutovinov A. A., Suleimanov B. F., Molkov S. V., Sunyaev R. A., 2004, *AstL*, 30, 772
- Revnivtsev M., Churazov E., Postnov K., Tsygankov S., 2009, *A&A*, 507, 1211
- Revnivtsev M., Sazonov S., Churazov E., Forman W., Vikhlinin A., Sunyaev R., 2009, *Natur*, 458, 1142
- Revnivtsev M., et al., 2010, *A&A*, 513, A63
- Ross R. R., Fabian A. C., 2005, *MNRAS*, 358, 211
- Sakano M., Warwick R. S., Decourchelle A., Wang Q. D., 2005, *MNRAS*, 357, 1211
- Sazonov S., Revnivtsev M., Gilfanov M., Churazov E., Sunyaev R., 2006, *A&A*, 450, 117
- Shakura N. I., Sunyaev R. A., 1973, *A&A*, 24, 337
- Singh K. P., White N. E., Drake S. A., 1996, *ApJ*, 456, 766
- Stacey W. S., Heinke C. O., Elsner R. F., Edmonds P. D., Weiskopf M. C., Grindlay J. E., 2011, *ApJ*, 732, 46
- Uttley P., McHardy I. M., Vaughan S., 2005, *MNRAS*, 359, 345
- Vaughan S., 2005, *A&A*, 431, 391
- Vaughan S., 2010, *MNRAS*, 402, 307
- Warner B., 1987, *MNRAS*, 227, 23
- Wijnands R., et al., 2006, *A&A*, 449, 1117
- Wu K., Cropper M., Ramsay G., Saxton C., Bridge C., 2003, *ChJAS*, 3, 235